

Cross-correlation between thermal Sunyaev-Zeldovich effect and the integrated Sachs-Wolfe effect

Cyril Creque-Sarbinowski¹, Simeon Bird², and Marc Kamionkowski²

¹*Department of Physics, Massachusetts Institute of Technology,
77 Massachusetts Avenue, Cambridge, MA 02139, USA*

²*Department of Physics and Astronomy, Johns Hopkins University,
3400 N. Charles Street, Baltimore, MD 21218, USA*

Large-angle fluctuations in the cosmic microwave background (CMB) temperature induced by the integrated Sachs-Wolfe (ISW) effect and Compton- y distortions from the thermal Sunyaev-Zeldovich (tSZ) effect are both due to line-of-sight density perturbations. Here we calculate the cross-correlation between these two signals. Measurement of this cross-correlation can be used to test the redshift distribution of the tSZ distortion, which has implications for the redshift at which astrophysical processes in clusters begin to operate. We also evaluate the detectability of a yT cross-correlation from exotic early-Universe sources in the presence of this late-time effect.

I. INTRODUCTION

The standard Λ CDM cosmological model provides a remarkably good fit to an array of precise measurements. However, there still remain some tensions between different measurements which must be resolved, and the physics responsible for the generation of primordial perturbations has yet to be delineated. This paper addresses both these issues.

Large-angle fluctuations in the cosmic microwave background (CMB) temperature (T) are induced not only by density perturbations at the CMB surface of last scatter (the Sachs-Wolfe effect; SW), but also by the growth of density perturbations along the line of sight (the integrated Sachs-Wolfe effect; ISW) [1]. Although the CMB frequency spectrum is very close to a blackbody, there are small distortions, of the Compton- y type, induced by the rare scattering of CMB photons from hot electrons in the intergalactic medium (IGM) of galaxy clusters [2]. This y distortion has been mapped, as a function of position on the sky, by Planck with an angular resolution of a fraction of a degree [3, 4], and there are vigorous discussions of future missions, such as PIXIE [5] and PRISM [6], that will map the y distortion with far greater sensitivity and resolution.

Given that both the tSZ and ISW fluctuations are induced by density perturbations at relatively low redshifts, there should be some cross-correlation between the two [7], and the purpose of this paper is to calculate this cross-correlation. The motivation for this work is two-fold: First, there is some tension between the measured amplitude of y fluctuations and the amplitude of density perturbations inferred from CMB measurements [8–11]. The tension, though, is based upon theoretical models that connect the y -distortion and density-perturbation amplitudes. Ingredients of these models include nonlinear evolution of primordial perturbations, gas dynamics, and feedback processes, all of which can become quite complicated. Any empirical handle on this physics would therefore be useful. To quantify how well the cross-correlation can constrain these processes, we introduce a param-

eter, ϵ , which describes the peak redshift of the cross-correlation signal. If clusters were to develop a hot envelope earlier than currently expected from theory, ϵ would increase. We design this parameter so that it does not affect the tSZ signal, merely the cross-correlation. Using our formalism we quantify how well the cross-correlation breaks the degeneracy between structure formation parameters (such as the amplitude of fluctuations, σ_8) and the astrophysical processes which lead to the halo pressure profile.

The second motivation involves the search for exotic early-Universe physics. Recent work has shown that primordial non-gaussianity may lead to a yT cross-correlation which may be used to probe scale-dependent non-gaussianity [12]. The present calculation will be used to explore whether this early-Universe signal can be distinguished from late-time effects that induce a yT correlation.

This paper is organized as follows. In Section II we derive expressions for the power spectra for the ISW effect, the tSZ effect, and their cross-correlation, and then present numerical results. In Section III we evaluate the prospects to infer some information about the redshift distribution for tSZ fluctuations from measurement of the tSZ-ISW cross-correlation. In Section IV we estimate the sensitivity of future measurements to the tSZ-ISW cross-correlation from primordial non-gaussianity. We conclude in Section V.

II. CALCULATION

A. The ISW Effect

The integrated Sachs-Wolfe (ISW) effect describes the frequency shift of CMB photons as they traverse through time-evolving gravitational potentials. The fractional temperature fluctuation in a direction \hat{n} due to this fre-

quency shift is

$$\frac{\Delta T}{T}(\hat{n}) = -\frac{2}{c^2} \int d\eta \frac{d\phi}{d\eta}(c\eta\hat{n}; z) = -\frac{2}{c^2} \int dz \frac{d\phi}{dz}(r\hat{n}; z), \quad (1)$$

where $\phi(\vec{x}, z)$ is the gravitational potential at position \vec{x} and redshift z , η the conformal time, c the speed of light, and r the distance along the line of sight.

The potential ϕ is related to the density perturbation through the Poisson equation $\nabla^2\phi = 4\pi G\rho$, where ∇ is a gradient with respect to physical position, G Newton's constant, and ρ the matter density. We write $\rho(\vec{x}; z) = \bar{\rho}[1 + \delta(\vec{x}; z)]$ in terms of the mean matter density $\bar{\rho}$ and fractional density perturbation $\delta(\vec{x}; z)$. We then use the Friedmann equation to write $\bar{\rho} = (3/8\pi G)\Omega_m H_0^2 a^{-3}$ in terms of the matter density Ω_m (in units of the critical density), Hubble parameter H_0 , and scale factor $a = (1+z)^{-1}$. We further write the density perturbation $\delta(\vec{x}; z) = D(z)\delta(\vec{x}; z=0)$ in terms of the linear-theory growth factor $D(z)$. We can then re-write the Poisson equation as

$$\phi(\vec{x}; z) = -\frac{3}{2}\Omega_m H_0^2 \frac{D(z)}{a(z)} [\nabla_c^{-2}\delta(\vec{x}; z=0)], \quad (2)$$

where $\nabla_c = \nabla/a$ is the gradient with respect to the moving coordinates.

The power spectrum for ISW-induced angular temperature fluctuations is then obtained using the Limber approximation, which can be stated as follows: If we observe a two-dimensional projection,

$$p(\hat{n}) = \int dr q(r)\delta(r\hat{n}), \quad (3)$$

of a three-dimensional field $\delta(\vec{x})$, with line-of-sight-distance weight function $q(r)$, then the angular power spectrum, for multipole l , of $p(\hat{n})$ is

$$C_l^p = \int dr \frac{[q(r)]^2}{r^2} P\left(\frac{l+1/2}{r}\right), \quad (4)$$

in terms of the three-dimensional power spectrum $P(k)$, for wavenumber k , for $\delta(\vec{x})$.

Using Eqs. (1), (2), and (4), we find the power spectrum for ISW-induced temperature fluctuations to be,

$$\begin{aligned} C_l &= \left(\frac{3\Omega_m H_0^2}{c^3(l+1/2)^2}\right)^2 c \int r^2 dr \left[H(z) \frac{d}{dz} \left(\frac{D(z)}{a(z)} \right) \right]^2 P(k) \\ &= \left(\frac{3\Omega_m H_0^2}{c^3(l+1/2)^2}\right)^2 \int c dz H(z) \left[r(z) \frac{d}{dz} \left(\frac{D(z)}{a(z)} \right) \right]^2 P(k) \text{ in terms of a transfer function,} \\ &= \int \frac{c dz}{H(z)} [\Delta_l^{\text{isw}}(z)]^2 P\left(\frac{l+1/2}{r}\right), \end{aligned} \quad (5)$$

in terms of the matter-density power spectrum $P(k)$ today. Note that we used the relation $dz = -(H/c)dr$ to get from the first to the second line in Eq. (5), and we have defined in the last line the ISW transfer function,

$$\Delta_l^{\text{isw}}(z) = \frac{3\Omega_m H_0^2}{c^3(l+1/2)^2} r(z) H(z) \frac{d}{dz} \left(\frac{D(z)}{a(z)} \right). \quad (6)$$

B. The Thermal Sunyaev-Zeldovich Effect

The thermal SZ effect (tSZ) arises from inverse-Compton scattering from the hot electrons in the intergalactic medium of galaxy clusters. This upscattering induces a frequency-dependent shift in the CMB intensity in direction \hat{n} which we write as a brightness-temperature fluctuation,

$$\left(\frac{\Delta T}{T}\right)_\nu(\hat{n}) = g(\nu)y \equiv \left(x \frac{e^x + 1}{e^x - 1} - 4\right) y(\hat{n}), \quad (7)$$

where $y(\hat{n})$ is the y distortion in direction \hat{n} , and $x \equiv h\nu/k_B T$, with ν the frequency, k_B the Boltzmann constant, h the Planck constant, and $T = 2.7255$ K the CMB temperature [13]. The Compton- y distortion is given by an integral,

$$y(\hat{n}) \equiv \frac{k_B \sigma_T}{m_e c^2} \int ds n_e(s\hat{n}) T_e(s\hat{n}), \quad (8)$$

along the line of sight, where s is the (physical) line-of-sight distance, σ_T the Thomson cross section, $n_e(\vec{x})$ the electron number density at position \vec{x} , and $T_e(\vec{x})$ the electron temperature. The hot electrons that give rise to this distortion are assumed to be housed in galaxy clusters with a variety of masses M and a variety of redshifts z . The spatial abundance of clusters with masses between M and $M + dM$ at redshift z is $(dn/dM)dM$ in terms of a mass function $(dn/dM)(M, z)$, a function of mass and redshift. Galaxy clusters of mass M at redshift z are distributed spatially with a fractional number-density perturbation that is assumed to be $b(M, z)\delta(\vec{x})$ in terms of a bias $b(M, z)$. The spatial fluctuations to the electron pressure $P_e(\vec{x}) = k_B n_e(\vec{x}) T_e(\vec{x})$ that give rise to angular fluctuations in the Compton- y parameter induced by clusters of mass M and redshift z can then be modeled as $b(M, z)$ times a convolution of the density perturbation $\delta(\vec{x})$ with the electron-pressure profile of the cluster. Since convolution in configuration space corresponds to multiplication in Fourier space, the Limber derivation discussed above can be used to find the power spectrum for angular fluctuations in the Compton- y parameter to be [3, 7, 14–16],

$$C_l^{yy, 2h} = \int \frac{c dz}{H(z)} [\Delta_l^y(z)]^2 P\left(\frac{l+1/2}{r}\right), \quad (9)$$

$$\Delta_l^y(z) = r(z) D(z) \int \frac{dn}{dM} dM y_l(M, z) b(M, z). \quad (10)$$

Here, $y_l(M, z)$ is the 2d Fourier transform of the Compton- y image, on the sky, of a cluster of mass M at redshift z and is given in terms of the electron pressure profile $P_e(M, z; x)$, as a function of scale radius x in the cluster. We neglect relativistic effects, which are second-order for our purposes [17]. We use for our numerical work the electron-pressure profiles of Ref. [18, 19] with

the parameters described in [20]. We assume the halo mass function of Ref. [22] and the halo bias of Ref. [23].

The “2h” superscript in the y -parameter power spectrum indicates that this is the “two-halo” contribution, the y autocorrelation that arises from large-scale density perturbations. There is an additional “one-halo” contribution that arises from Poisson fluctuations in the number of clusters. This is [21],

$$C_l^{yy,1h} = \int dz [r(z)]^2 \frac{c}{H(z)} \int dM \frac{dn(M, z)}{dM} |y_l(M, z)|^2. \quad (11)$$

The total y -parameter power spectrum is $C_l^{yy} = C_l^{yy,1h} + C_l^{yy,2h}$. To avoid our signal being dominated by unphysical $z \sim 0$ objects, we place a lower integration limit of $z = 0.02$, the redshift of the COMA cluster.

C. ISW-tSZ cross-correlation

Given that the temperature fluctuation induced by the ISW effect and the two-halo contribution to tSZ fluctuations are both generated on large angular scales by the same fractional density perturbation $\delta(\vec{x})$, there should be a cross-correlation between the two. From the expressions, Eq. (5) and (9), it is clear that this cross-correlation is

$$C_l^{yT} = \int \frac{cdz}{H(z)} \Delta_l^{\text{isw}}(z) \Delta_l^y(z) P\left(\frac{l+1/2}{r}\right). \quad (12)$$

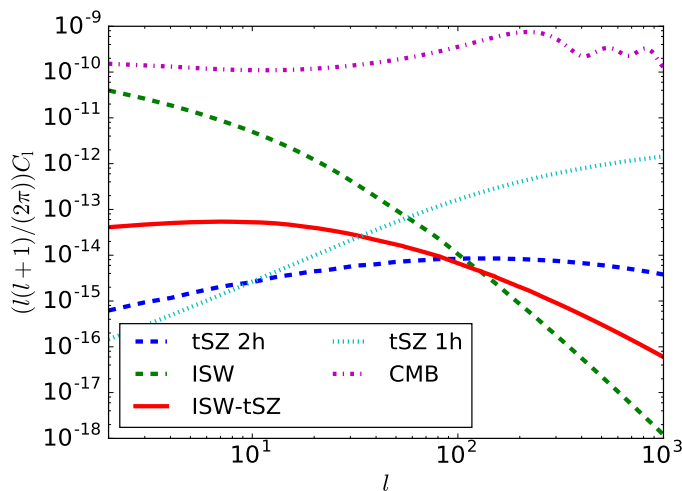


FIG. 1. The ISW power spectrum C_l^{isw} (green) and the two-halo contribution ($y, 2h$) to C_l^{yy} (blue) are shown in dashed lines, while C_l^{yT} is shown in solid red. The one-halo contribution ($y, 1h$) to C_l^{yy} is dotted. The CMB power spectrum is shown dot-dashed for comparison.

D. Numerical results and approximations

Fig. 1 shows the resulting power spectra. For our numerical results, we use a vacuum-energy density (in units of critical) $\Omega_\Lambda = 0.721$, matter density $\Omega_m = 0.279$, baryon density $\Omega_b = 0.046$, a critical density for collapse of $\delta_c = 1.686$, and dimensionless Hubble parameter $h = 0.701$, although the large-angle results that will be our primary focus are largely insensitive to these details. In practice, we find that over ninety percent of the contribution comes from the redshift range $z = 0 - 3$ and the halo mass range $10^{13} M_\odot$ and $10^{15} M_\odot$. We therefore integrate over slightly wider ranges; $z = 0.02 - 4$ and halo mass $10^{12} M_\odot$ and $10^{16} M_\odot$.

The large angle (low- l) behaviors of the ISW-ISW autocorrelation, the yT cross-correlation, and the one- and two-halo contributions to the yy power spectra are easy to understand qualitatively. Let us begin with the ISW effect. Here, the l dependence of the transfer function is $\Delta_l^{\text{isw}} \propto l^{-2}$, and for large angles ($l \lesssim 20$), the power spectrum is $P(l/r) \propto l$, assuming $l + 1/2 \approx l$. As a result, $l^2 C_l^{\text{isw}} \propto l^{-1}$ for $l \lesssim 20$. Next consider the tSZ power spectra. Galaxy clusters subtend a broad distribution of angular sizes but are rarely wider than a degree. Thus, for $l \lesssim 20$, they are effectively point sources. The Fourier transform is thus effectively approximated by $y_l(M, z) \simeq y_{l=0}(M, z)$ which is itself precisely the integral of the y -distortion over the cluster image on the sky, or equivalently, the total contribution of the cluster to the angle-averaged y . As a result of the independence of y_l on l and $P(l/r) \propto l$ for $l \lesssim 20$, we infer $l^2 C_l^{yy,2h} \propto l$ and $l^2 C_l^{yT} \propto \text{const}$ for $l \lesssim 20$. Finally, the one-halo contribution to C_l^{yy} is nearly constant (i.e., $l^2 C_l \propto l^2$) for $l \lesssim 20$ as expected for Poisson fluctuations in what are (at these angular scales) effectively point sources.

III. SZ REDSHIFT DISTRIBUTION

We now discuss the prospects to learn about the redshift distribution of the galaxy clusters that produce the Compton- y distortion. As seen above, the yT correlation is significant primarily at multipole moments $l \lesssim 100$, where the window function $y_l(z)$ is largely independent of l . The amplitude of the cross-correlation, relative to the auto-correlations, can be largely understood by examining the overlap between the redshift dependences of the two transfer functions $\Delta_l^y(z)$ and $\Delta_l^{\text{isw}}(z)$. These transfer functions are shown in Fig. 2. More precisely, we plot—noting that $P(l/r) \propto l/r$ for the relevant angular scales— $\Delta_l / [H(z)r(z)]^{1/2}$, the square root of the integrands for C_l , as it is the overlap of these two functions that determines the strength of the cross-correlation relative to the auto-correlation. We also normalize the curves in Fig. 2 to both have the same area under the curve.

Given the current fairly precise constraints to dark-

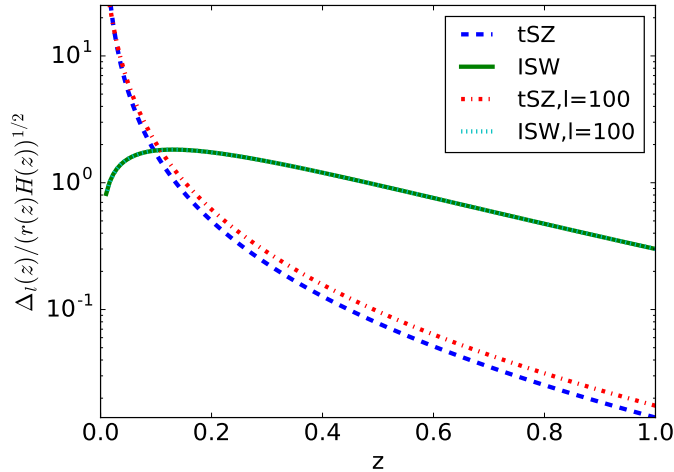


FIG. 2. We plot the transfer functions $\Delta_l^{\text{isw}}(z)$ and $\Delta_l^y(z)$, divided by $[r(z)H(z)]^{1/2}$, at $l = 20$. The squares of the plotted quantities are the redshift (z) integrands for the ISW power spectrum C_l^{isw} and the two-halo contribution to the tSZ power spectrum C_l^{yy} . Both curves are normalized so that the areas under the curve are the same. The tSZ-ISW cross-correlation C_l^{yT} is obtained from the overlap of these two.

energy parameters, the predictions for $\Delta_l^{\text{isw}}(z)$ has relatively small uncertainties. The prediction for $\Delta_l^y(z)$ depends, however, on the redshift distribution of the halo mass function, bias parameters, and cluster pressure profiles, all of which involve quite uncertain physics. Measurement of the yT correlation will, however, provide an additional empirical constraint on the redshift evolution of the y parameter.

To see how this might work, we replace

$$\Delta_l^y(z) \rightarrow \Delta_l^y(z) [1 + \epsilon(z - z_0)], \quad (13)$$

where

$$z_0 = \frac{\int \frac{dz}{r(z)H(z)} z \Delta_l^y(z)}{\int \frac{dz}{r(z)H(z)} \Delta_l^y(z)} \simeq 0.04 \left(\frac{l}{100} \right). \quad (14)$$

The functional form in Eq. (13), is chosen so that, with z_0 given in Eq. (14), the auto-correlation power spectrum C_l^{yy} will remain unaltered for small ϵ . This alteration thus describes, for $\epsilon > 0$, a weighting of the Compton- y distribution to smaller redshifts (and *vice versa* for $\epsilon < 0$) in such a way that leaves the total y signal unchanged.

We now estimate the smallest value σ_ϵ of ϵ that will be detectable with future measurements. This is given by

$$\frac{1}{\sigma_\epsilon^2} \simeq \sum_l \frac{(\partial C_l^{yT} / \partial \epsilon)^2}{(\sigma_l^{yT})^2}, \quad (15)$$

where

$$\frac{\partial C_l^{yT}}{\partial \epsilon} = \int \frac{cdz}{H(z)} \Delta_l^{\text{isw}}(z) \Delta_l^y(z) (z - z_0) P(l/r). \quad (16)$$

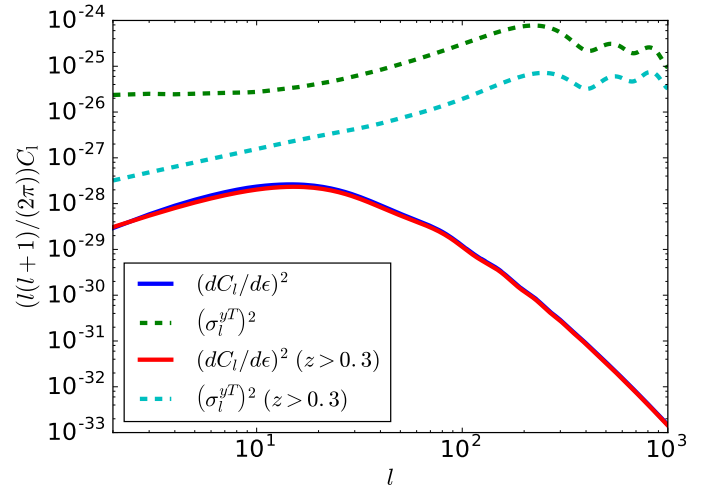


FIG. 3. The derivative $\partial C_l^{yT} / \partial \epsilon$ of the ISW-tSZ cross-correlation with respect to ϵ (solid blue), and the ISW-tSZ noise σ_l^{yT} (dashed green). We also show the same quantities restricting to $z > 0.3$ (solid red and dashed cyan, respectively), which substantially increases the signal-to-noise.

Fig. 3 shows $\partial C_l^{yT} / \partial \epsilon$ and σ_l^{yT} .

The error with which each C_l^{yT} can be determined is

$$(\sigma_l^{yT})^2 = \frac{1}{2l+1} \left[(C_l^{yT})^2 + C_l^{TT} (C_l^{yy} + N_l W_l^{-2}) \right], \quad (17)$$

where C_l^{TT} is the CMB temperature power spectrum, $W_l = e^{-l^2 \sigma_b^2 / 2}$ is a window function, and $N_l = (4\pi/N) \sigma_y^2$ is the noise in the measurement of C_l^{yy} . Here, σ_b the beam size and, σ_y the root-variance of the y -distortion measurement in each pixel, and N the number of pixels.

The Planck satellite has now measured the tSZ power spectrum and found good agreement with the expectations from the one-halo contribution to C_l^{yy} . They have now even presented good evidence for detection of the two-halo contribution at $l \lesssim 10$. From this we infer that the noise contribution N_l to the yy measurement is already small compared with C_l^{yy} , and it will be negligible for future experiments like PIXIE or PRISM. We also note from the numerical results that $(C_l^{yT})^2$ is small compared with $C_l^{yy} C_l^{TT}$ —this makes sense given that the cross-correlation of y with the ISW effect is small and further that the ISW effect provides only a small contribution to large-angle temperature fluctuations. We may thus approximate

$$(\sigma_l^{yT})^2 \simeq \frac{1}{2l+1} C_l^{TT} C_l^{yy}. \quad (18)$$

The smallest detectable value of ϵ evaluates to $\sigma_\epsilon \simeq 2.3$, for $z_0 = 0.13$. This is still a considerable uncertainty, but the signal to noise can be increased. While the majority of the cross-correlation signal is at low redshifts, the 1-halo tSZ term, which appears as noise in Eq. (17), peaks

even more strongly at low redshift. Thus the lowest-redshift bins are substantially noise dominated.¹ If we remove all information at redshifts $z < 0.3$, possible by explicitly detecting resolved clusters and masking them from the tSZ map, then the noise can be considerably reduced. In this case, the smallest detectable value becomes $\sigma_\epsilon \simeq 0.57$, which, if achieved, would provide some valuable information on the redshift distribution of tSZ fluctuations, constraining the formation of massive clusters to the era of dark energy dominance.

We also considered the profile of Ref. [21], which produces a larger tSZ signal and thus a larger cross-correlation. However, since the 1-halo tSZ term dominates the noise, this actually slightly decreased the sensitivity. Thus our results should be largely insensitive to the electron pressure profile used.

IV. PRIMORDIAL NON-GAUSSIANITY

We now review the yT cross-correlation from the scale-dependent primordial non-gaussianity scenario of Ref. [12]. If primordial perturbations are non-gaussian, the amplitude of small-wavelength power can be modulated by long-wavelength Fourier modes of the density field. The dissipation of primordial Fourier modes with wavenumbers $k \simeq 1 - 50 \text{ Mpc}^{-1}$ (which takes place at redshifts $1100 \lesssim z \lesssim 5 \times 10^4$) gives rise to primordial Compton- y distortions. If there is non-gaussianity, then the angular distribution of this y distortion may be correlated with the large-scale density modes that give rise, through the Sachs-Wolfe effect, to large-angle fluctuations in the CMB temperature.

The predictions for this primordial yT correlation depend on the yet-unmeasured isotropic value $\langle y \rangle$ of the Compton- y parameter for which we take as a canonical value 4×10^{-9} . The yy and yT power spectra for the scenario are then,

$$l^2 C_l^{yy,\text{ng}} \simeq 5.5 \times 10^{-20} \left(\frac{f_{\text{nl}}^y}{200} \right)^2 \left(\frac{\langle y \rangle}{4 \times 10^{-9}} \right)^2, \quad (19)$$

$$l^2 C_l^{yT,\text{ng}} \simeq 5.8 \times 10^{-15} \left(\frac{f_{\text{nl}}^y}{200} \right) \left(\frac{\langle y \rangle}{4 \times 10^{-9}} \right). \quad (20)$$

Here, f_{nl}^y is the non-gaussianity parameter for squeezed bispectrum configurations in which the wavenumber of the long-wavelength mode is of the $\sim \text{Gpc}^{-1}$ scales of modes that contribute to the ISW effect, while the two short-wavelength modes have wavelengths $1 \text{ Mpc}^{-1} \lesssim k \lesssim 50 \text{ Mpc}^{-1}$. As discussed in Ref. [12], there are no existing model-independent constraints on f_{nl}^y .

We now estimate the detectability of the yT cross-correlation from non-gaussianity, discussed in Ref. [12]. In that work, the late-time contribution to C_l^{yy} and C_l^{yT} was neglected, and the detectability of the primordial signal inferred assuming that detection of y fluctuations was noise-limited. Here we re-do those estimates taking into account the late-time yT correlation calculated above.

If the late-time yT is somehow known precisely, the signal-to-noise with which an early-Universe yT signal with power spectrum $C_l^{yT,\text{ng}}$ can be distinguished from the null hypothesis is

$$\left(\frac{S}{N} \right) = \left(\sum_l \frac{\left(C_l^{yT,\text{ng}} \right)^2}{\left(\sigma_l^{yT} \right)^2} \right)^{1/2}. \quad (21)$$

Using Eq. (18) and the numerical results for C_l^{yy} , we then obtain a signal-to-noise $(S/N) \simeq (f_{\text{nl}}^y/1065) \langle y \rangle / 4 \times 10^{-9}$. This calculation differs from that of Ref. [12] in two respects; we have included the late-time contribution to Compton- y fluctuations, which degrades the detectability f_{nl}^y by about a factor of 4, even if the late-time yT correlation is assumed to be known precisely. The detectability is, moreover, limited by cosmic variance and not from measurement noise. We have included in the sum in Eq. (21) angular modes up to $l \leq 1000$; the signal-to-noise improves if the sum is extended to higher l .

This calculation overestimates the smallest detectable signal, as there is a theoretical uncertainty in the late-time yT correlation, as discussed in Section III; it must instead be determined from the data. There is thus an additional uncertainty to the inferred value of f_{nl}^y that will arise after marginalizing over the uncertain late-time yT amplitude. We thus assume that the total yT power spectrum is a combination $C_l^{yT,\text{tot}} = \alpha C_l^{yT} + C_l^{yT,\text{ng}}$ of the late-time and non-gaussian contributions. Here $\alpha \sim 1$ accounts for uncertainty in the amplitude of yT . We then calculate the Fisher matrix [24],

$$F_{ij} = \sum_\ell \frac{\left(\partial C_\ell^{yT,\text{tot}} / \partial s_i \right) \left(\partial C_\ell^{yT,\text{tot}} / \partial s_j \right)}{\left(\sigma_\ell^{yT} \right)^2}, \quad (22)$$

where $\mathbf{s} = \{f_{\text{nl}}^y, \alpha\}$ is the set of parameters to be determined from the data, and the partial derivatives are evaluated under the null hypothesis $f_{\text{nl}} = 0$ and $\alpha = 1$. The noise with which f_{nl}^y can be determined, after marginalizing over α , is then $\left[(F^{-1})_{f_{\text{nl}}^y f_{\text{nl}}^y} \right]^{1/2}$ and the signal-to-noise (S/N) is f_{nl}^y divided by this quantity. Numerically, we find $(S/N) \simeq (f_{\text{nl}}^y/1100) \langle y \rangle / 4 \times 10^{-9}$. Thus, the marginalization over the ISW-tSZ effect only slightly decreases the detectability.

Since the noise is again dominated by the tSZ 1-halo term, we can perform a similar cleaning to low-redshift sources to that used in Section III. If we remove all $z < 0.3$ clusters, we find that we can detect a smaller value of f_{nl}^y . Numerically, using the Fisher matrix as above

¹ Eq. 17 assumes Gaussian fluctuations for C_l^{yy} . This assumption is invalid at $z \sim 0$, where a single nearby large cluster can dominate large angular scales. The $z \sim 0$ signal is already extremely small, however, so this does not change our conclusions.

to marginalise over uncertainty in the yT amplitude, we find $(S/N) \simeq (f_{\text{nl}}^y/400)(\langle y \rangle / 4 \times 10^{-9})$, closer to the value estimated in Ref. [12].

V. CONCLUSION

Here we have calculated the tSZ-ISW cross-correlation, investigated its use in constraining the redshift distribution of y -parameter fluctuations, and evaluated the detectability of an early-Universe yT cross-correlation. We showed that measurement of the yT cross-correlation can be used to constrain the redshift distribution of the sources of y -parameter fluctuations, as long as low-redshift tSZ clusters can be masked, something that may be of utility given uncertainties in the cluster-physics and large-scale-structure ingredients (pressure profiles, halo

biases, mass functions) that determine these fluctuations. We also showed that estimates, that neglect the yT correlations induced at late times, of the detectability of early-Universe yT correlations may be optimistic by factors of a few.

ACKNOWLEDGMENTS

We thank Liang Dai, Yacine Ali-Haïmoud, and Ely Kovetz for useful discussions. We also thank the anonymous referee for a very quick and conscientious report. SB was supported by NASA through Einstein Postdoctoral Fellowship Award Number PF5-160133. This work was supported by NSF Grant No. 0244990, NASA NNX15AB18G, the John Templeton Foundation, and the Simons Foundation.

-
- [1] R. K. Sachs and A. M. Wolfe, *Astrophys. J.* **147**, 73 (1967) [*Gen. Rel. Grav.* **39**, 1929 (2007)].
 - [2] R. A. Sunyaev and Y. B. Zeldovich, *Comments Astrophys. Space Phys.* **4**, 173 (1972).
 - [3] P. A. R. Ade *et al.* [Planck Collaboration], *Astron. Astrophys.* **571**, A21 (2014) [arXiv:1303.5081 [astro-ph.CO]].
 - [4] N. Aghanim *et al.* [Planck Collaboration], arXiv:1502.01596 [astro-ph.CO].
 - [5] A. Kogut *et al.*, *JCAP* **1107**, 025 (2011) [arXiv:1105.2044 [astro-ph.CO]].
 - [6] P. André *et al.* [PRISM Collaboration], *JCAP* **1402**, 006 (2014) [arXiv:1310.1554 [astro-ph.CO]].
 - [7] N. Taburet, C. Hernandez-Monteagudo, N. Aghanim, M. Douspis and R. A. Sunyaev, *Mon. Not. Roy. Astron. Soc.* **418**, 2207 (2011) [arXiv:1012.5036 [astro-ph.CO]].
 - [8] M. Lueker *et al.*, *Astrophys. J.* **719**, 1045 (2010) [arXiv:0912.4317 [astro-ph.CO]].
 - [9] E. Komatsu *et al.* [WMAP Collaboration], *Astrophys. J. Suppl.* **192**, 18 (2011) [arXiv:1001.4538 [astro-ph.CO]].
 - [10] P. A. R. Ade *et al.* [Planck Collaboration], *Astron. Astrophys.* **571**, A20 (2014) [arXiv:1303.5080 [astro-ph.CO]].
 - [11] P. A. R. Ade *et al.* [Planck Collaboration], arXiv:1502.01597 [astro-ph.CO].
 - [12] R. Emami, E. Dimastrogiovanni, J. Chluba and M. Kamionkowski, *Phys. Rev. D* **91**, 123531 (2015) [arXiv:1504.00675 [astro-ph.CO]].
 - [13] D. J. Fixsen, *Astrophys. J.* **707**, 916 (2009) [arXiv:0911.1955].
 - [14] E. Komatsu and T. Kitayama, *Astrophys. J.* **526**, L1 (1999) [astro-ph/9908087].
 - [15] J. M. Diego and S. Majumdar, *Mon. Not. Roy. Astron. Soc.* **352**, 993 (2004) [astro-ph/0402449].
 - [16] P. A. R. Ade *et al.* [Planck Collaboration], *Astron. Astrophys.* **581**, A14 (2015) [arXiv:1502.00543 [astro-ph.CO]].
 - [17] N. Itoh, Y. Kohyama and S. Nozawa, *Astrophys. J.* **502**, 7 (1998) doi:10.1086/305876 [astro-ph/9712289].
 - [18] D. Nagai, A. V. Kravtsov and A. Vikhlinin, *Astrophys. J.* **668**, 1 (2007) doi:10.1086/521328 [astro-ph/0703661].
 - [19] M. Arnaud, G. W. Pratt, R. Piffaretti, H. Boehringer, J. H. Croston and E. Pointecouteau, *Astron. Astrophys.* **517**, A92 (2010) doi:10.1051/0004-6361/200913416 [arXiv:0910.1234 [astro-ph.CO]].
 - [20] K. Dolag, E. Komatsu and R. Sunyaev, arXiv:1509.05134 [astro-ph.CO].
 - [21] E. Komatsu and U. Seljak, *Mon. Not. Roy. Astron. Soc.* **336**, 1256 (2002) [astro-ph/0205468].
 - [22] J. L. Tinker *et al.*, *Astrophys. J.* **688**, 709 (2008) [arXiv:0803.2706 [astro-ph]].
 - [23] R. K. Sheth and G. Tormen, *Mon. Not. Roy. Astron. Soc.* **308**, 119 (1999) [astro-ph/9901122].
 - [24] G. Jungman, M. Kamionkowski, A. Kosowsky and D. N. Spergel, *Phys. Rev. D* **54**, 1332 (1996) doi:10.1103/PhysRevD.54.1332 [astro-ph/9512139].